A SYNOPSIS

ON

"DESIGN, SYNTHESIS AND BIOLOGICAL EVALUATION OF SOME NOVEL HETEROCYCLIC COMPOUNDS AS ANTI-ALZHEIMER'S AGENTS"

By

Joshi Karan Divyesh

Research Guide

Dr. Prashant R. Murumkar

Pharmacy Department

Faculty of Pharmacy, Kalabhavan Campus,

The Maharaja Sayajirao University of Baroda,

Vadodara-390001

1. Introduction

Alzheimer's disease (AD) is a chronic neurodegenerative disease that starts slowly and with time gets worsen [1-2]. It should be described by, and later named after, a German psychiatrist and pathologist Alois Alzheimer in 1906 [3]. The most common types of dementia, about 60-70% are caused due to Alzheimer's. Common symptoms include difficulty in remembering followed by problems with language, disorientation, mood swings, loss of motivation and behavioral issues in the later stages as the disease progresses. Gradually, the body functions are lost leading to death [4]. The rate of progression of the disease may vary, generally having the life expectancy of about 3-9 years [5-6]. Non-communicable diseases now make up 7 of the world's top 10 causes of death, according to WHO's report in Global Health Estimates, wherein Alzheimer's disease and other forms of dementia are now among leading causes of death globally, ranking 3rd after cardiovascular diseases and diabetes.

Although the disease is poorly understood, it is believed that about 70% of the risk is inherited from genes. Other risk factors involve head injury, depression and hypertension [7]. Moreover, examination of brain tissue is essential for confirmation of the disease, a credible diagnosis is done on the basis of illness, patient history and cognitive testing with medical imaging and blood tests to rule out other possible causes [8].To decrease the risk of AD, generally mental and physical exercise is recommended as there are no suitable medications or supplements which can reduce the risk of the occurrence of AD [9].

1.1. Rates of dementia

Worldwide, around 50 million people have dementia, with nearly 60% living in low- and middle-income countries. Every year, there are nearly 10 million new cases and is projected to reach 82 million in 2030 and 152 million by 2050. Much of this increase is attributable to the rising numbers of people with dementia living in low- and middle-income countries including India therefore it is extremely important to address the same. [10-11]

1.2. Social and economic impact

Alzheimer's disease has significant social and economic implications in terms of direct medical and social care costs, and the costs of informal care. In 2015, the total global societal cost of

dementia was estimated to be US$ 818 billion, equivalent to 1.1% of global gross domestic product (GDP). The total cost as a proportion of GDP varied from 0.2% in low- and middle-income countries to 1.4% in high-income countries therefore, it was observed that second and third world countries overlook mental health issues which lead to direct impact on wellbeing of the population.

1.3. Scenario in India

Advances in the medical field have been associated with increase in life expectancy leading to increasing number of old age population. As per the 2011 census, India is home to about 65 million people of age 65 and above, constituting 5.5% of the total population which is going to increase drastically in the next 20 years. Prevalence of dementia in India is reported to be 2.7% and so as the age increase, prevalence of Alzheimer's increases. Unlike the West, in India most of the elderly people live with their families and most patients with dementia are taken care of by the families. With the increasing elderly population and reducing joint family system in our country, Alzheimer's poses a great challenge in future.

The real problem lies in the management of Alzheimer's disease. In the last 25 years, the biological groundwork of AD has been unraveled, but no disease-modifying agent has been discovered. Considering the lower prevalence and incidence of AD as compared to that in western countries, long-term research plan to identify the protective factors and subsequent research application in animals and human should be urgently undertaken as mainstream Indian population will enter into 60's in coming years and so it would be extremely difficult then to control the situation which is undermined right now in the current scenario.

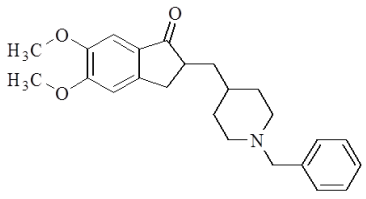

Donepezil

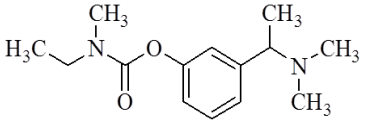

Rivastigmine

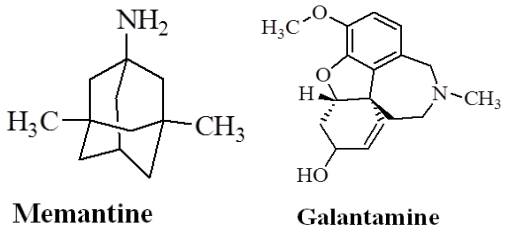

Memantine **Galantamine**

Fig 1: Marketed drugs approved by USFDA

2. Treatment

There is no as such cure for `AD, where the available treatments offer relatively small symptomatic benefit but still remains analgesic in nature. The current treatments available can be classified into pharmaceuticals, psychological and caregiving. Currently, there are four primary therapeutic option approved by USFDA to treat the cognitive problems of AD wherein, three are acetyl cholinesterase inhibitors (galantamine, rivastigmine and donepezil) while one N-methyl-D-aspartate (NMDA) receptor blocker (memantine). As the disease is multifactorial, no medication has shown to delay or halt the progression of the disease [12]. These treatments are mainly effective in treating mild cognitive impairments providing temporary relief from symptoms; however, they fail to cure or reverse the progression of AD. Therefore, it is important to focus on developing molecules which actually address ailment of the disease by either prolonging the time of occurrence of Alzheimer's or treating the disease rather than simply giving symptomatic relief to the patient.

3. Pathophysiology of AD:

3.1. Role of cholinesterase in AD

Literature review showed that the neuritic amyloid plaques and neurofibrillary tangles (NFT) which comprise of hyperphosphorylated tau proteins represent the basic neuropathology of AD. [13,14] AD is characterized by low concentration levels of acetylcholine (Ach) in the hippocampus and cortex owing to dysfunction in the system of the cholinergic neurotransmission on the nervous system (CNS).[15] The cholinergic system regulates the memory and learning of the individual, in which two enzymes has role in the depletion of ACh levels, acetyl cholinesterase (AChE) and butryl cholinesterase (BuChE).[16] Therefore, these two enzymes are identified as the

most potential targets for the treatment of AD, glaucoma, myasthenia gravis and in the recovery of victims of nerve gas exposure.[17]

The key component of the cholinergic nervous system and the neuromuscular junctions which play role in the neurotransmission of the central nervous system and the termination of the signals in the nerve endings is AChE. [18] While BuChE is synthesized in the liver and enriched in the circulation, the exact physiology of the enzyme is still unknown and is generally is viewed as backup for the homologous AChE. [19,20] Since the activity of the of AChE decreases progressively in certain areas of brain with progress of the AD from mild to severe stages, the BuChE levels remains either unchanged or increases by 20%, thereby increasing the amount of BuChE in neurons and neuritic plaques.

Out of all the pathophysiology that are discussed for the AD, it is known from the literature that the most common and prominent aspect is the increase of AChE and BuChE activity in the diseased patients which leads to decreased neuronal transmission along with increase in the Aβ amyloid plaques in the brain leading death of neuronal cells thereby causing loss of memory and other disorder.[21-24] When we discuss about the AChE enzyme structure, it is supposed to have two active site the CAS (catalytic active site) and PAS (peripheral active site). The CAS site happen to have two subsites, a negatively charged/ anionic site and an esteratic site [25] while the PAS is another anionic site which is located around 14A° away from the CAS. [26]

3.2. Role of Choline acetyltransferase (ChAT) in AD

Choline acetyltransferase (commonly abbreviated as ChAT, but sometimes CAT) is a transferase enzyme responsible for the synthesis of the neurotransmitter acetylcholine. ChAT catalyzes the transfer of an acetyl group from the coenzyme acetyl-CoA to choline, yielding acetylcholine (ACh). ChAT is found in high concentration in cholinergic neurons, both in the central nervous system (CNS) and peripheral nervous system (PNS). As with most nerve terminal proteins, ChAT is produced in the body of the neuron and is transported to the nerve terminal, where its concentration is highest. Presence of ChAT in a nerve cell classifies this cell as a "cholinergic" neuron. In humans, the choline acetyltransferase enzyme is encoded by the CHAT gene. [27]

The Alzheimer's disease (AD) involves difficulty in memory and cognition. The concentrations of acetylcholine and ChAT are remarkably reduced in the cerebral neocortex and hippocampus. [28] Although the cellular loss and dysfunction of the cholinergic neurons is considered a contributor to Alzheimer disease, it is generally not considered as a primary factor in the development of this disease. It is proposed that the aggregation and deposition of the Beta amyloid protein, interferes with the metabolism of neurons and further damages the cholinergic axons in the cortex and cholinergic neurons in the basal forebrain. [29]

3.3. **Role of MAO-B in Alzheimer's**

Monoamine oxidase B, also known as MAOB, is an enzyme that in humans is encoded by the MAOB gene. The protein encoded by this gene belongs to the flavin monoamine oxidase family. It is an enzyme located in the outer mitochondrial membrane. It catalyzes the oxidative deamination of biogenic and xenobiotic amines and plays an important role in the catabolism of neuroactive and vasoactive amines in the central nervous system and peripheral tissues (such as dopamine). This protein preferentially degrades benzylamine and phenethylamine. Similarly to monoamine oxidase A (MAOA), it also degrades dopamine.

Alzheimer's disease (AD) and Parkinson's disease (PD) are both associated with elevated levels of MAO-B in the brain. The normal activity of MAO-B creates reactive oxygen species, which directly damage cells. MAO-B levels have been found to increase with age, suggesting a role in natural age related cognitive decline and the increased likelihood of developing neurological diseases later in life. More active polymorphisms of the MAO-B gene have been linked to negative emotionality, and suspected as an underlying factor in depression. Activity of MAO-B has also been shown to play a role in stress-induced cardiac damage. Over-expression and increased levels of MAO-B in the brain have also been linked to the accumulation of amyloid β-peptides (Aβ), through mechanisms of the amyloid precursor protein secretase, γ-secretase, responsible for the development of plaques, observed in Alzheimer's and Parkinson's patients. Evidence suggests that siRNA silencing of MAO-B, or inhibition of MAO-B through MAOI-B (Selegline, Rasagiline), slows the progression, improves and reverses the symptoms, associated with AD and PD, including the reduction of Aβ plaques in the brain.

4. Literature Review

Neurodegenerative diseases are characterized by the progressive loss of structure, function, and quantity of neurons, which result in clinical syndromes including motor, cognitive, and behavioral decline. Currently, Alzheimer's disease (AD), is reported as the top neurodegenerative diseases, and is associated with abnormal protein aggregations within the brain. Although academic institutions and pharmaceutical industries have dedicated tremendous efforts to developing drug candidates for treating this disease, unfortunately, an effective therapeutic has not been identified yet. Patients and their families continue to bear a huge economic burden as well as enduring physical and emotional pressure. Meanwhile, diverse small-molecule drug candidates have been explored as potential therapeutics for AD. In the development of potential drug candidates for the treatment of AD, pyrazole scaffolds have two intrinsic advantages. First, the pyrazole heterocycle is a bidentate ligand: it can act as both a hydrogen-bond donor and a hydrogen-bond acceptor at the same time, thus allowing it to interact with carbonyl oxygen and amide proton on the peptide backbone complementarily. Second, π–π-stacking interaction between pyrazole and phenylalanine in β-sheet peptides amplifies their high affinity toward peptide backbones.

With respect to their corresponding protein targets, the leading pyrazole-containing therapeutic compounds can be divided into five classes: (1) acetylcholinesterase (AChE) inhibitors; (2) protein aggregation inhibitors; (3) PDE inhibitors; (4) dual leucine zipper kinase inhibitors; and (5) monoamine oxidase B inhibitors (MAO-B).

❖ Compounds showing potential AChE and BuChE inhibitory activity

In 2018, Turkan et al. reported a series of substituted pyrazol-4-yl-diazene derivatives, and *in vitro* enzymatic assay suggested that all were effective AChE and BuChE inhibitors with Ki values at the nanomole level, better than tacrine **[1]**, a discontinued acetylcholinesterase inhibitor that was used to treat AD [30]. However, their poor selectivity between AChE and BuChE, and broad activities over α-glycosidase and cytosolic carbonic anhydrase might be problematic. Shaikh et al. reported novel scaffolds of N-substituted pyrazole-derived α-aminophosphonates, two of these compounds **[2,3]** exhibited strong potency against AChE and high selectivity over BuChE, and their performances were better than the commercially available drugs galantamine and rivastigmine [31]. Gutti et al. reported a linear pyrazole derivative **[4]** as an AChE inhibitor in 2019 [32]. When

tested in MC65 cells at 50 μM, compound **[4]** improved cell viability by 90% and could reduce Aβ1–42 aggregation induced by metals effectively at 20 μM.

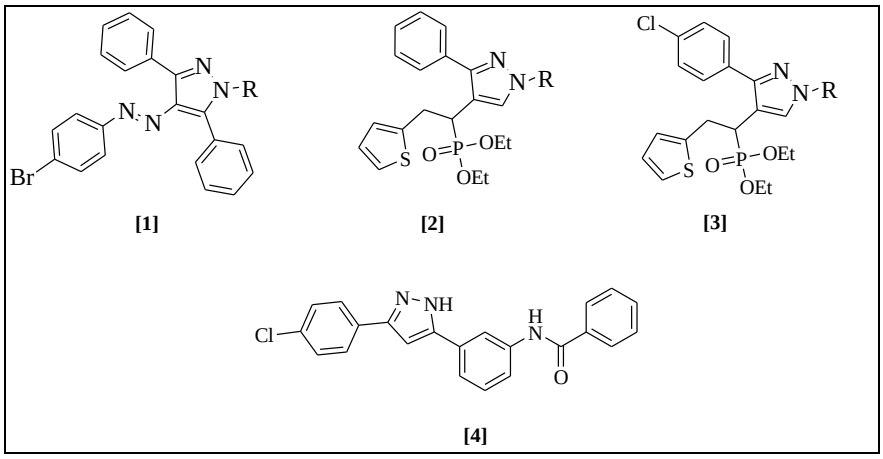

❖ **Compounds showing potential Protein Aggregation Inhibitory activity**

In 2011, Hochdörffer et al. developed a series of $A\beta_{42}$ inhibitors based on a trimeric aminopyrazole carboxylic acid framework. They could convert well-ordered fibrils into less structured aggregates and thin bent filaments through backbone recognition and hydrophobic interactions with $A\beta_{42}$ [33]. Compound (Trimer-TEG-Lys-OMe, **[5]**) displayed the most potent inhibition and disaggregation activities against fibril formation, with ~80% of reduced thioflavin fluorescence absorption and 43% of increased PC-12 cell viability in an Aβ existing cytotoxic environment. Notably, the triethyleneglycol (TEG) spacer bridging trimeric aminopyrazole core and lysine appendix are essential to maintain the inhibition activity, as the spacer plays an active role in destabilizing the U-shaped turn of the Aβ protofilament. When the spacer was omitted **[6]**, an accelerated aggregation was contrarily observed. Meanwhile, the attached extension (TEG-Lys-OMe, **[5]**) allows diversity; when it was replaced by a pentapeptide "LPFFD", the corresponding new compound showed a substoichiometric IC_{50} value (3 μM). Considering that Aβ concentration is at nanomolar range in the brain, much lower than the concentration (10 μM) used in in vitro studies, a 3 μM IC_{50} value is remarkable.

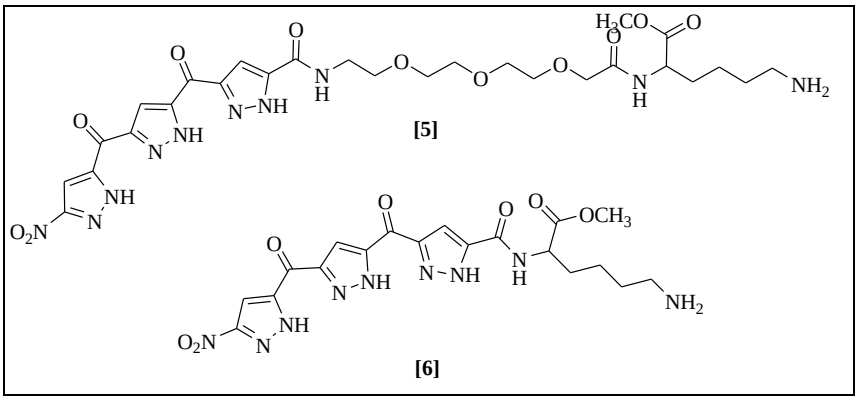

Anle138b **[7]** was first identified as a potent α-synuclein aggregation inhibitor when it was administered in vivo at nanomolar concentrations [34]. Later in vitro and in vivo studies carried in mouse models of AD suggested that it could also inhibit the formation of pathological tau aggregates by specifically binding to pre-aggregated tau species [35]. Molecular dynamic (MD) simulations revealed that anle138b **[7]** could block the conversion of ordered antiparallel β-strands into disordered β-sheet rich conformations by preferentially interacting with pre-aggregated tau fragments to reduce the overall number of intermolecular hydrogen bonds [36]. Structure-activity analysis showed that the pyrazole scaffold plays a crucial role in anle138b's inhibitory effect; when the pyrazole moiety was replaced by imidazole (sery345, **[8]**) or isoxazole (sery338, **[9]**), the anti-aggregation effect was weakened due to altered hydrogen bond characteristics. Interestingly, pyrazole anle234b **[10]**, a structural isomer of anle138b, is biologically inactive. Anle234b **[10]** is more sterically hindered than anle138b due to placement of the bulky bromine group at the ortho- rather than meta-position, which creates a more stable/less flexible conformation. The torsional inactivation of anle234b **[10]** hampers the interactions of the bromophenyl and pyrazole ring with peptide backbones, resulting in a reduced hydrogen bond strength.

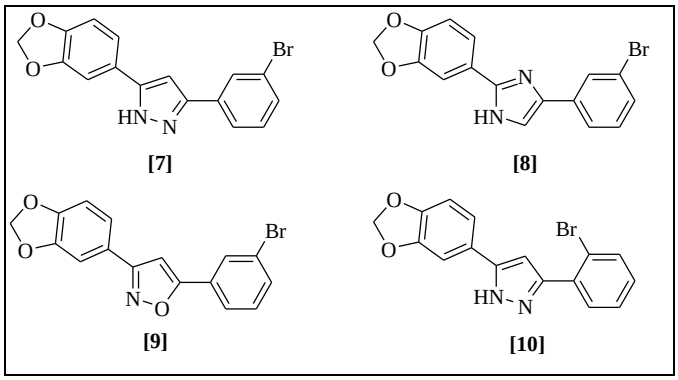

❖ **Compounds showing potential Phosphodiesterase (PDE) Inhibitory activity**

PDE9A is primarily expressed in the brain, with high concentrations in the cerebellum, neocortex, striatum, and hippocampus [37]. Consistent with the specific function of cGMP in controlling neurotransmission and enhancing hippocampal synaptic plasticity, the inhibition of PDE9A results in significant accumulation of cGMP in cerebrospinal fluid of nonhuman primates and humans, thus damaging brain functions like sensory processing, learning, and memory [38]. Compound PF-04447943 **[11]** (K_i = 8.3 nM), a PDE9A inhibitor developed by Pfizer, was found to increase cGMP concentration in cerebrospinal fluid by ~23-fold when dosed in rats, monkeys, and humans [39]. Unfortunately, no cognitive improvement was observed in subsequent phase II clinical trials when administered twice a day for 12 weeks to moderate stage AD patients. Instead, it resulted in a higher incidence of serious adverse events compared to the placebo group [40]. BI 409306 **[12]** is another potent PDE9A inhibitor, and has IC_{50} values of 65 nM and 168 nM in human and rat, respectively [41,42]. Preclinical studies demonstrated that BI 409306 (183) could increase cGMP concentrations in rodent prefrontal cortex and cerebrospinal fluid, and promoted long-term potentiation, and improved episodic and working memory performance [42]. Although it was well tolerated in prodromal to mild stage AD patients, its phase II clinical trial was discontinued because no visible efficacy in improving cognitive function was observed [42].

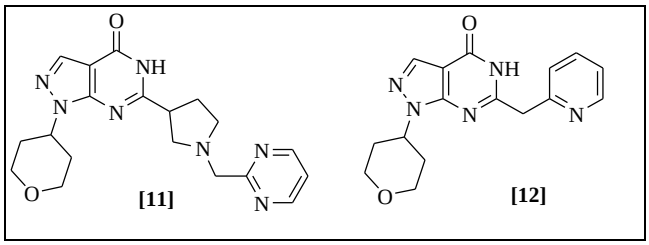

❖ **Compounds showing potential Monoamine oxidase B inhibitory activity (MAO-B)**

A new strategy for tackling the complexity of AD pathology is incorporating several pharmacological scaffolds into a single molecular entity to produce a synergistic effect [43]. This tactic turned out to be useful when fusing pharmacological scaffolds from a MAO-B inhibitor and an AChE inhibitor together to afford multi-target-directed lead compounds as potential therapeutics against AD [44,45]. Tzvvetkov et al. reported three potent, reversible, and competitive MAO-B inhibitors **[13-15]** with high selectivity against the MAO-A isoform [46]. Enzyme studies suggest

that all of them have the ability to bind to Fe(II) and Fe (III) via UV–Vis. These water-soluble, highly blood–brain barrier permeable MAO-B inhibitors are promising drug and radioligand candidates as diagnostic and therapeutic agents for AD.

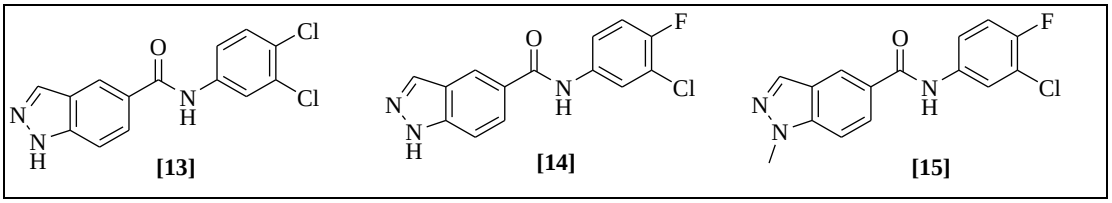

[13] **[14]** **[15]**

5. Aim and Objectives

- Design and synthesis of novel vicinal diaryl pyrazole derivatives **(I)** as potent anti-Alzheimer's agents.
- To establish the method for the synthesis of intermediates and proposed compounds.
- To confirm the structures of the synthesized compounds by IR, ^{1H}-NMR, MS analysis.
- To evaluate the proposed compounds for their anti-Alzheimer's activity.

6. Rationale of Design

- Previous research work from our laboratory which includes

1. Shidore M, Machhi J, Shingala K, Murumkar P, Sharma MK, Agrawal N, Tripathi A, Parikh Z, Pillai P, Yadav MR. Benzylpiperidine-linked diarylthiazoles as potential anti-Alzheimer's agents: synthesis and biological evaluation. Journal of medicinal chemistry. 2016 Jun 23;59(12):5823-46.
   AChE IC_{50} value of 0.30 ± 0.01 μM & BuChE 1.84 ± 0.03 μM
2. Sinha A, Tamboli RS, Seth B, Kanhed AM, Tiwari SK, Agarwal S, Nair S, Giridhar R, Chaturvedi RK, Yadav MR. Neuroprotective role of novel triazine derivatives by activating Wnt/β catenin signaling pathway in rodent models of Alzheimer's disease. Molecular neurobiology. 2015 Aug;52(1):638-52.
   $A\beta_{1-42}$ IC_{50} value of 5 μM
3. Sinha A, Tamboli RS, Seth B, Kanhed AM, Tiwari SK, Agarwal S, Nair S, Giridhar R, Chaturvedi RK, Yadav MR. Correction to: Neuroprotective Role of Novel Triazine Derivatives by Activating Wnt/β Catenin Signaling Pathway in Rodent Models of Alzheimer's Disease. Molecular neurobiology. 2019 Oct 1;56(10):7246-8.

$A\beta_{1-42}$ IC_{50} value of 5 µM, clearly suggest that vicinal diaryltriazine and vicinal diarylthiazole show potential anti-cholinesterase activity interact with the PAS site of the cholinesterase enzyme whereas the substituted benzylpiperidine moiety, an active pharmacophore of the donepezil binds to the CAS site of the cholinesterase receptor.

- Based on the results of previous research work and literature survey, we thought it will be logical to develop new series of vicinal diaryl pyrazole analogs **(Compound I)** as multi-target directed ligands having potential anti-Alzheimer's activity because pyrazole is reported for its diverse activities in AD and has shown activities in nanomolar concentration. Moreover, there are no evident toxicity reports of pyrazole as scaffold unlike drugs like tacrine so it was rational in choosing pyrazole for designing.

The designed **compound [I]** is shown in **Figure 2.**

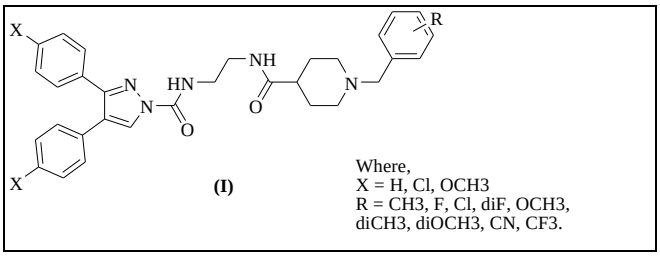

Fig 2: Designed **compound 1**

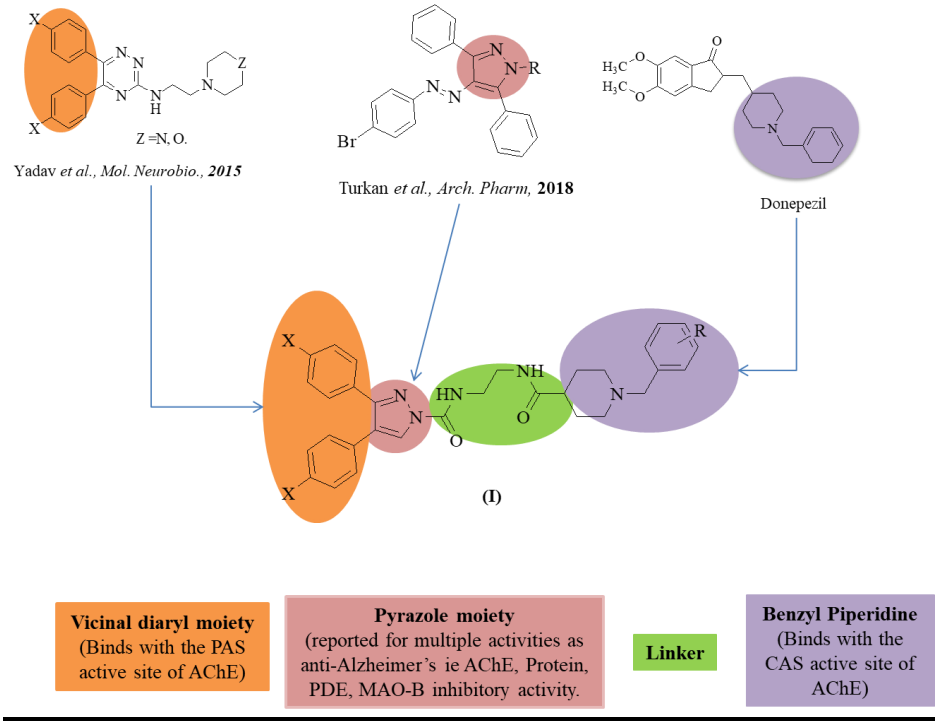

- According to **Compound I,** we thought of deigning **compound 2,** having a vicinal diaryl heterocycle, along with a pyrazole moiety which is now attached to a carbamate functional group which is very well known for its anti-AD activity that is already reported in the standard marketed drug rivastigmine used in the treatment for Alzheimer's disease.
- The designed **compound [II]** is shown in **Figure 3.**

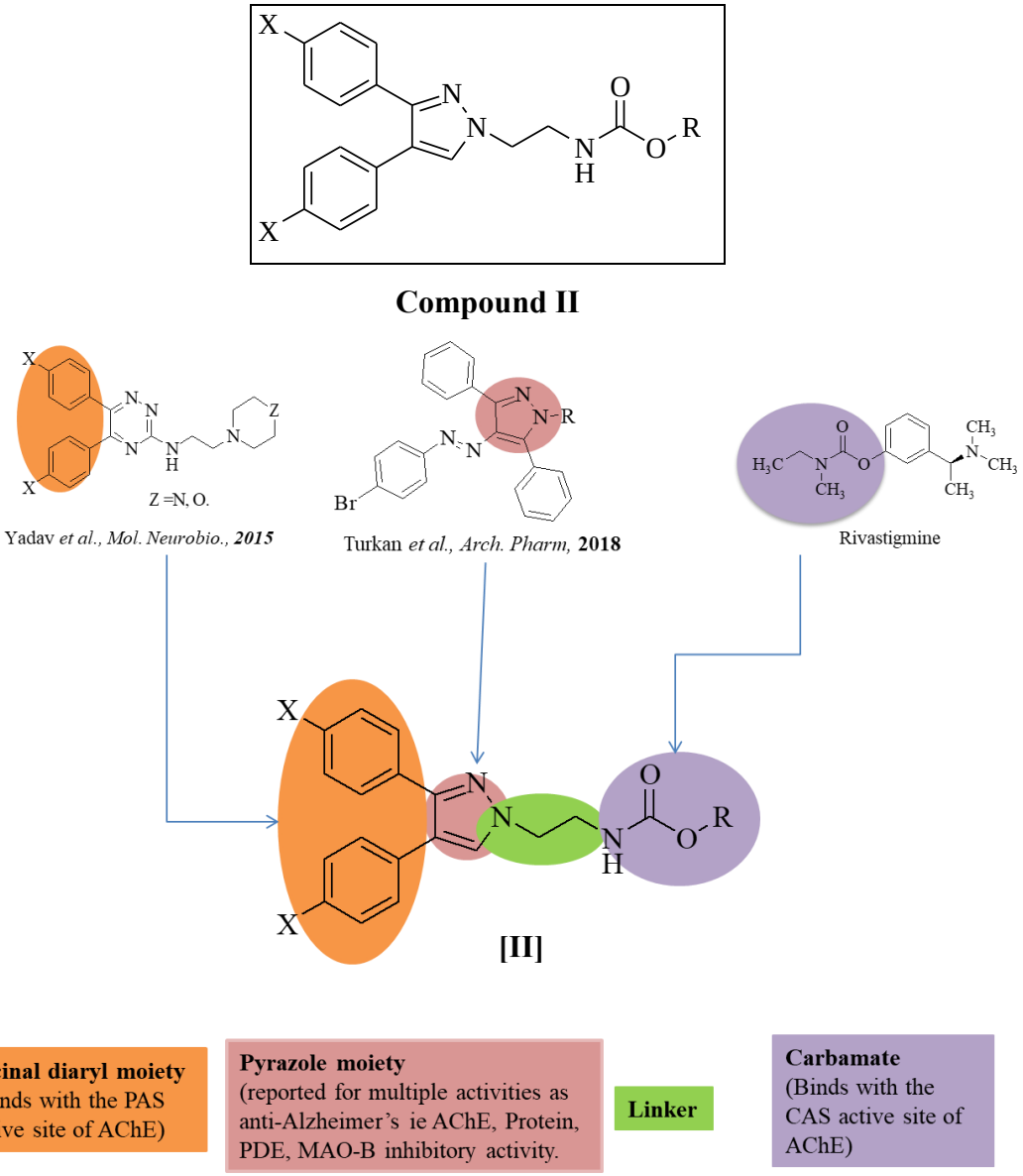

Figure 3: Designing of **Compound II**

7. General scheme for the synthesis of Compound I and II:

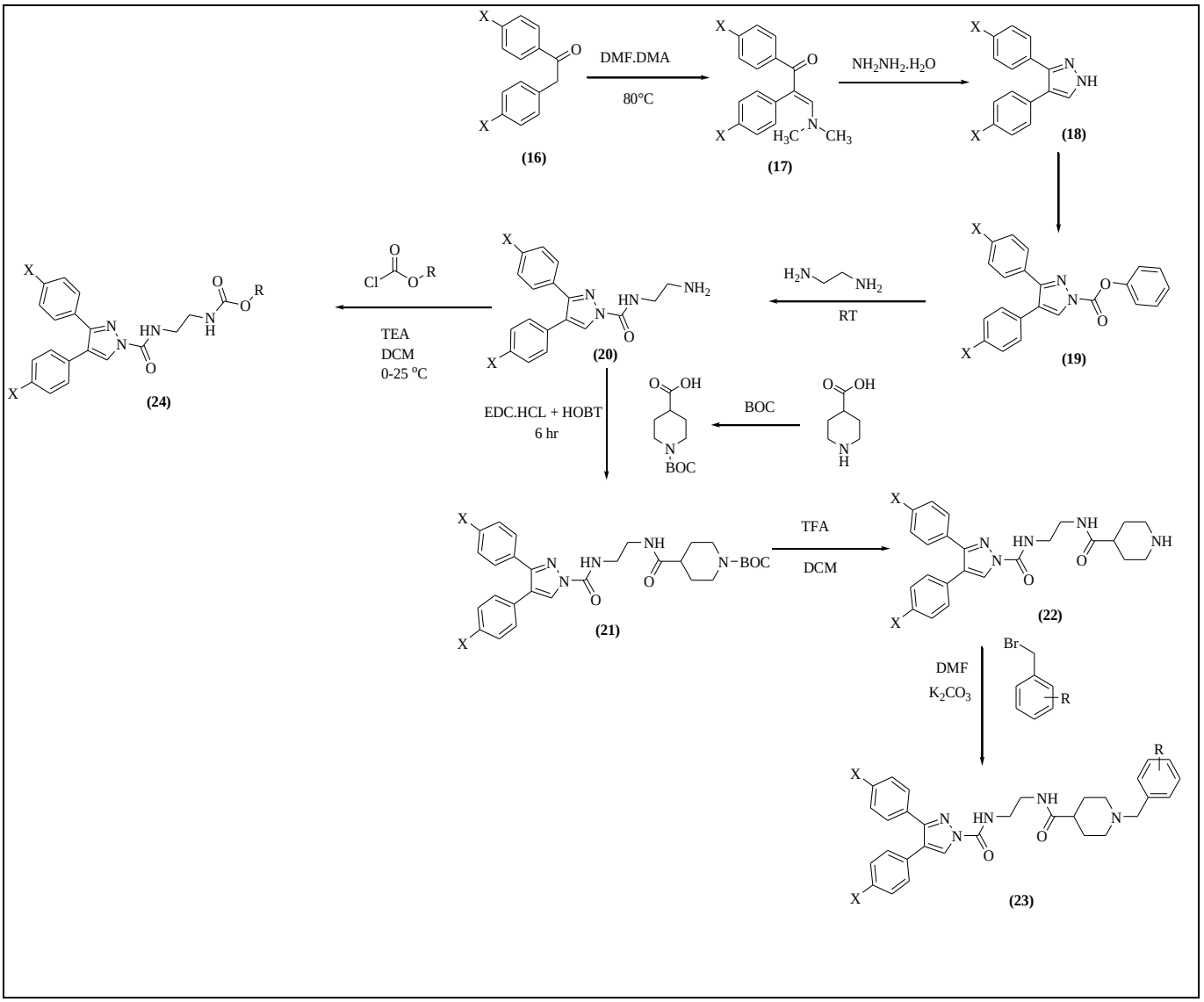

8. Result and Discussion:

Designed prototype **23 & 24 (Compound I and II)** synthesized using following procedure and as depicted in synthetic scheme:

Procedure for the synthesis of 1,2-Bis(4-methoxyphenyl)ethanone (16)

In 50 ml RBF, 2-(4-methoxyphenyl)acetic acid (1 gm, 6.01 mM) was reacted with thionyl chloride (1.74 ml, 24.07 mM) at reflux condition for 2-3 hrs in vacuum sealed and dry condition. Completion of the reaction was monitored by TLC. After completion of the reaction, fumes of HCl and gaseous by-products were removed by vacuum. In another 100 ml RBF, anhydrous aluminium chloride (1.20 gm, 9.02 mM) was taken in dry DCM at 0-4 °C and anisole (0.65 ml, 6.01 mM) was

added to it. To this reaction mixture 2-(4-methoxy phenyl) acetyl chloride in dry DCM was added slowly drop-wise in cold condition. The reaction mixture was then allowed to stir for 2 hrs. After completion of the reaction, the reaction mixture was poured into crushed ice containing conc. HCl. The mixture was then extracted with chloroform (30 ml X 3) and the combined organic layer was washed with $NaHCO_3$ solution (5%, aqueous). The organic layer was dried over anhydrous Na_2SO_4 and removed to obtain the desired product (**16**). IR (KBr, cm^{-1}) aromatic -CH stretching shown at 3028, aliphatic -CH stretching at 2963, -C=O ketone at 1674, and -OCH_3 ether bending at 1256.

Procedure for the synthesis of *(E)*-3-(dimethylamino)-1,2-*Bis*(4-methoxyphenyl)prop-2-en-1-one (17)

1,2-*Bis*(4-methoxyphenyl)ethanone was refluxed with DMF.DMA (dimethylformamide dimethylacetal) for 16 hr at 80^o C with constant stirring. The reaction mixture was monitored by TLC till the completion reaction completion. Then, the mixture was allowed to cool down to room temperature in which n-hexane was poured. After that, the mixture was further cooled down/refrigerated in order to solidify the product. Finally, a yellow crystalline was obtained after cooling it for 3-4 hrs. The reaction mixture was filtered and the n-hexane solvent was removed. Product was dried and packed. IR (KBr, cm^{-1}) aromatic -CH stretching shown at 3029, aliphatic -CH stretching at 2963, -C=O ketone at 1653, and -OCH_3 ether bending at 1246.

Procedure for the synthesis of 3,4-*Bis*(4-methoxyphenyl)-*1H*-pyrazole (18)

(E)-3-(dimethylamino)-1,2-*Bis*(4-methoxyphenyl)prop-2-en-1-one **(17)** was taken in clean, dry RBF and methanol was added. Hydrazine hydrate was added and the reaction mixture was allowed to reflux for 3 hrs. Excess of methanol was distilled off and the reaction mixture was poured into ice cold water. The precipitates were filtered in vacuum and dried and packed. The mass analysis showed peak at (*m/z*) 281 $[M+H]^+$ and IR (KBr, cm^{-1}) -NH stretching 3342, -C-N stretching at 1590, -OCH_3 bending at 1248.

Procedure for the synthesis of Phenyl 3,4-Bis(4-methoxyphenyl)-1H-pyrazole-1-carboxylate (19)

3,4-*Bis*(4-methoxyphenyl)-*1H*-pyrazole **(18)** was taken in a clean dry RBF and dry DCM was added and stirred in ice till temperature attained 0-5 °C. Triethylamine was added in the reaction mixture followed by slow addition of phenyl chloroformate. The reaction mixture was

stirred for 1 hr and TLC was monitored. The reaction was poured into ice cold water and extracted with $CHCl_3$ (25ml x 3). The organic layer was combined, dried over Na_2SO_4 and evaporated. The obtained product was taken as it for the next step. The mass data showed peak at (*m/z*) 401 $[M+H]^+$ and the IR data showed peak carbamate -C=O stretching at 1745, -C-N stretching at 1590 and ether -OCH_3 1248 cm^{-1}.

Procedure for the synthesis of N-(2-aminoethyl)-3,4-Bis(4-methoxyphenyl)-1H-pyrazole-1-carboxamide (20)

Phenyl 3,4-*Bis*(4-methoxyphenyl)-*1H*-pyrazole-1-carboxylate (**19**) was taken in clean, dry RBF and dry DCM was added. Ethylene diamine was added in the reaction and was allowed to stir. The reaction was monitored with TLC. After completion of reaction, DCM was removed and the reaction mixture was poured in ice cold water to obtain solid product The precipitate so obtained was further purified by column chromatography using $CHCl_3$: MeOH (10%) as mobile phase to get the desired product as pale-yellow solid. The mass data showed peak at (*m/z*) 367 $[M+H]^+$ and IR spectra suggested amide stretching at 1638 cm^{-1}.

Procedure for the synthesis of t.butyl 4-(2-(4,5-bis(4-methoxyphenyl)pyrimidin-2-ylamino)ethyl- carbamoyl)piperidine-1-carboxylate (21)

In a two necked RBF, 1-(*t*.butoxycarbonyl)piperidine-4-carboxylic acid was dissolved in dry DCM (25 ml) at 0-4 ^{o} C under a stream of nitrogen gas. To this, 1-ethyl-3-(3-dimethylaminopropyl)carbodiimide hydrochloride (EDC.HCl) and hydroxybenzotriazole (HOBt) were added and the reaction mixture was stirred at 0-4 ^{o}C for 30 min. Anhydrous triethylamine was then added to the reaction mixture followed by N-(2-aminoethyl)-3,4-*Bis*(4-methoxyphenyl)-*1H*-pyrazole-1-carboxamide **(20)**. The reaction mixture was allowed to stir for 12 hrs at rt. After completion of the reaction, excess of DCM was evaporated on rota and the remaining reaction mixture was poured in ice cold water to get a solid. The solid was filtered, washed with water and dried to afford the desired product as a pale yellow solid (200, 1.42 gm, 88%). The mass data showed peak at (*m/z*) 579 $[M+2H]^+$

Procedure for the synthesis of compound 22:

In a 25 ml RBF, *t*.butyl 4-(2-(4,5-bis(4-methoxyphenyl)pyrimidin-2-ylamino)ethyl-carbamoyl)piperidine-1-carboxylate **(21)** (1 gm, 1.77 mM) was dissolved in DCM (4 ml) and a

mixture of 1ml 4M HCl in dioxan was added and stirred for 2 hrs below 5°C. DCM was removed and diethyl ether was added slowly to the reaction mixture at cold conditions with continuous stirring to get solid which was filtered and dried to obtain desired product as a yellow semisolid.

Procedure for the synthesis of *N*-(2-(3,4-bis(4-methoxyphenyl)-1*H*-pyrazole-1-carboxamido)ethyl)-1-benzylpiperidine-4-carboxamide 23:

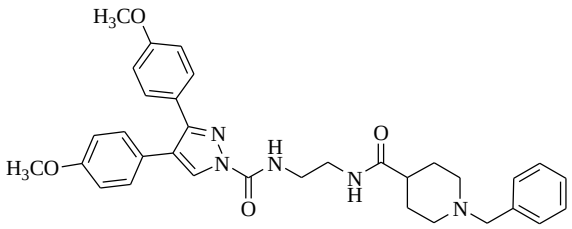

N-(2-(3,4-bis(4-methoxyphenyl)-1*H*-pyrazole-1-carboxamido)ethyl)-1-benzylpiperidine-4-carboxamide

(23)

In a 25ml clean, dry RBF, compound **22** (0.5g, 0.86mM) was added to 10 ml of dry DCM, and triethylamine (0.362 ml, 2.5mM) was added. Benzyl bromide (0.102 ml, 0.86mM) was added and the reaction mixture was stirred till reaction was completed. After completion of reaction, the reaction mixture was poured into cold water. The precipitated solid was filtered, dried and purified through column chromatography using $CHCl_3$: CH_3OH (10%) as mobile phase to obtain the desired product as a white solid (**8**, 0.35 gm). The mass spectra showed *m/z* 568 $[M+H]^+$. PMR spectra of compound 23 showed singlet peak of pyrazole ring proton at δ 8.19 followed by triplet amide proton at 7.55, two aromatic ortho position doublet proton of the phenyl ring at 7.44 & 7.43, four aromatic protons doublet at 7.29, multiplet three aromatic protons at 7.26 – 7.17, four aromatic protons at 6.87 & 6.85, triplet broad amide proton at 6.25 (t, J = 5.2 Hz, 1H), six aliphatic -OCH_3 protons at 3.81, four multiplet protons of the spacer between 3.61 – 3.56 & 3.52-3.47, and nine aliphatic -CH protons of the piperidine ring between 2.90-1.72.

Procedure for the synthesis of isobutyl 2-(3,4-bis(4-methoxyphenyl)-1H-pyrazole-1-carboxamido)ethylcarbamate 24:

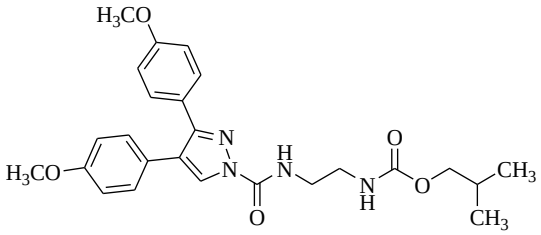

isobutyl 2-(3,4-bis(4-methoxyphenyl)-1*H*-pyrazole-1-carboxamido)ethylcarbamate

In a 25ml clean, dry RBF, compound 20 (0.5g, 0.86mM) was added to 10 ml of dry DCM, and triethylamine (0.362 ml, 2.5mM) was added. Chilling was applied and isobutyl chloroformate (0.205 ml, 1.03mM) was added and the reaction mixture was stirred till reaction was completed. After completion of reaction, the reaction mixture was poured into cold water. The precipitated solid was filtered, dried and purified through column chromatography using n Hexane: Ethyl Acetate (30%) as mobile phase to obtain the desired product as a white solid (**24**, 0.35 gm). In the PMR spectra, one singlet proton of aromatic -CH of the pyrazole ring was at 8.21 followed by broad singlet of carbamate amide -NH at 7.50. Aromatic 8 protons between 7.45-6.85 were found followed by one broad singlet of amide -NH at 5.08. The aliphatic doublet -CH_2 of isobutyl present at 3.85, six -OCH_3 present at 3.82 followed by 4 protons of -CH_2 spacer two-two each present between 3.60-3.43. One triplet proton of the isobutyl 1.89 and six -CH_3 protons of isobutyl at 0.9.

9. Biological Evaluation

Biological work is being carried out at Karolinska Institutet, Sweden. Results are awaited.

Following biological activity for the proposed synthesized compounds are carried:

a) *In-vitro* AChE and BuChE activities using Ellman's

AssayPrinciple: DTNB reacts with a free sulfhydryl group to yield a mixed disulfide and 2-nitro-5-thiobenzoic acid (TNB; see Figure 2). The target of DTNB in this reaction is the conjugate base (R—S-) of a free sulfhydryl group. TNB is the "colored" species produced in this reaction and has a high molar extinction coefficient in the visible range. The molar extinction coefficient of TNB is reported to be 13,600 M-1cm-1 at 412 nm and pH 8.0.

b) **Thioflavin-T assay:**

Thioflavin T (ThT) is a benzothiazole salt obtained by the methylation ofdehydrothiotoluidine with methanol in the presence of hydrochloric acid. ThT is used as a dye to visualize and quantify

the presence or fibrilization of misfolded protein aggregates, or amyloid, both in vitro and in vivo (e.g.,plaques composed of amyloid beta found in the brains of Alzheimer's disease patients; plaques of PrP fibrils found in brains of CGD patients).

The Thioflavin T (ThT) Assay measures changes of influorescence intensity of ThT upon binding to amyloid fibrils. The enhanced fluorescence can be observed by fluorescence microscopy or by fluorescent spectroscopy. The spectroscopic assay is commonly used to monitor fibrilization over time, but the assay is not strictly quantitative and differences in binding have been observed for samples after lyophilization.

c) *In-vitro* DPPH for determination of anti-oxidant activity:

DPPH (2,2-diphenyl-1-picryl-hydrazyl-hydrate) free radical method is an antioxidant assay based on electron-transfer that produces a violet solution in ethanol. This free radical, stable at room temperature, is reduced in the presence of an antioxidant molecule, giving rise to colourless ethanol solution.

d) Free radical scavenging activity:

Over time ROS, generated from the thermal decomposition of AAPH, will quench the signal from the fluorescent probe fluorescein. The subsequent addition of an antioxidant produces a more stable fluorescence signal, with signal stability depending on the antioxidant's capacity. The data points are summarized over the time by the evaluation software. This is then compared to the standard, Trolox®, and is expressed as micromoles of Trolox® equivalents (TE) per gram or per milliliter of sample (µmole of TE/g or µmole of TE/mL) taken up to 120 minutes.

e) *In-Vitro* Blood-Brain Barrier Permeation Assay and Drug-Likeness Evaluation

Parallel artificial membrane permeability assay (**PAMPA**) is a method which determines the permeability of substances from a donor compartment, through a lipid-infused artificial membrane into an acceptor compartment. A multi-well microtitre plate is used for the donor and a membrane/acceptor compartment is placed on top; the whole assembly is commonly referred to as a "sandwich". At the beginning of the test, the drug is added to the donor compartment, and the acceptor compartment is drug-free. After an incubation period which may include stirring, the sandwich is separated and the amount of drug is measured in each compartment. Mass balance allows calculation of drug that remains in the membrane.

10. References:

1. Burns A, Iliffe S., Alzheimer's disease*; British Medicinal Journal*, **2009,** *338*, 158.
2. "Dementia Fact sheet". World Health Organization. 12 December **2017.**
3. Berchtold NC, Cotman CW; Evolution in the conceptualization of dementia and Alzheimer's disease: Greco-Roman period to the 1960s; *Neurobiology of aging,* **1998,** *19,*173–89.
4. Querfurth HW, LaFerla FM, Alzheimer's disease, *New England Journal of Medicine,* **2010**, *362 (4),* 329-44.
5. Todd S, Barr S, Roberts M, Passmore AP, Survival in dementia and predictors of mortality: a review, *International Journal of Geriatric*, **2013,** *28 (11),* 1109-24.
6. Ballard C, Gauthier S, Corbett A, Brayne C, Aarsland D, Jones E, Alzheimer's disease, *Lancet*, **2011,** *377 (9770),* 1019-31.
7. “Dementia diagnosis and assessment”, National Institute for Health and Care Excellence (NICE), **2014**.
8. Hsu D, Marshall GA., Primary and Secondary Prevention Trials in Alzheimer Disease: Looking Back, Moving Forward, *Current Alzheimer Research*, **2017,** *14 (4),* 426-40.
9. Disease Injury Incidence Prevalence Collaborators, Global, regional, and national incidence, prevalence, and years lived with disability for 310 diseases and injuries, 1990-2015: a systematic analysis for the Global Burden of Disease Study, *Lancet,* **2015**, *388 (10053),* 1545–1602.
10. Disease Injury Incidence Prevalence Collaborators, Global, regional, and national incidence, prevalence, and years lived with disability for 249 diseases and injuries, 1990-2015: a systematic analysis for the Global Burden of Disease Study, *Lancet* **2015**, *388 (10053),* 1459–1544.
11. Larson EB, Shadlen MF, Wang L, McCormick WC, Bowen JD, Teri L, Kukull WA, Survival after initial diagnosis of Alzheimer disease, *Annals of Internal Medicine*, **2004**, *140 (7)*, 501–09.
12. Bilkei-Gorzo A, The endocannabinoid system in normal and pathological brain ageing, *Philosophical* Transactions of the Royal Society of London. *Series B, Biological Sciences*, **2012**, *367 (1607)*, 3326–41.
13. Barnes, N. M.; Neumaier, J. F. Neuronal 5-HT receptors and SERT. *Tocris Bioscience Review*, **2014**, *34*, 1-15.
14. Kimura, Y.; Naitou, Y.; Wanibuchi, F.; Yamaguchi, T. 5-HT(2C) receptor activation is a common mechanism on proerectile effects of apomorphine, oxytocin and melanotanII in rats. *European. Journal of Pharmacology*, **2008**, *589*, 157-162.

15. Finberg, J. P.; Vardi, Y. Inhibitory effect of 5-hydroxytryptamine on penile erectile function in the rat. *British Journal of Pharmacology*, **1990**, *101*, 698-702.
16. Esen, A. A.; Gidener, S.; Guler, C.; Guven, H.; Kirkali, Z. Contractility changes of the deep dorsal penile vein due to serotonin. *Journal of Urology*, **1997**, *158*, 234-237.
17. Feijo Fde, M.; Bertoluci, M. C.; Reis, C. [Serotonin and hypothalamic control of hunger: a review, *Revista da Associacao Medica Brasillieria*, **2011**, *57*, 74-77.
18. Bishop, M. J.; Nilsson, B. M. New 5-HT2C receptor agonists; *Expert. Opin. Ther. Pat*, **2003**, *13*, 1691-1705.
19. O'Neil, R. Role of the 5HT2C receptor in regulation of metabolism and mesolimbic dopamine. *Vanderbilt Review Neuroscience*, **2010**, *2*, 19-24.
20. Dubin, A. E.; Huvar, R.; D'Andrea, M. R.; Pyati, J.; Zhu, J. Y.; Joy, K. C.; Wilson, S. J.; Galindo, J. E.; Glass, C. A.; Luo, L.; Jackson, M. R.; Lovenberg, T. W.; Erlander, M. G. The pharmacological and functional characteristics of the serotonin 5-HT(3A) receptor are specifically modified by a 5-HT(3B) receptor subunit. *Journal of Biological Chemistry*, **1999**, *274*, 30799-30810.
21. Kim, G. W.; Lin, J. E.; Valentino, M. A.; Colon-Gonzalez, F.; Waldman, S. A. Regulation of appetite to treat obesity. *Expert Review in Clinical Pharmacology*, **2011**, *4*, 243-259.
22. Brobeck, J. R. Mechanism of the development of obesity in animals with hypothalamic lesions. *Physiological Review*, **1946**, *26*, 541-559.
23. Anand, B. K.; Brobeck, J. R. Hypothalamic control of food intake in rats and cats. Yale *Journal of Biological Chemistry*, **1951**, *24*, 123-140.
24. Joseph, A. K.; Lawrence, R. M. Process for producing anorexia. *US 3253989* A, **1966**.
25. Nilsson, B. M. 5-Hydroxytryptamine2C (5-HT2C) receptor agonists as potential antiobesity agents. *Journal of Medicinal Chemistry*, **2006**, *49*, 4023-4034.
26. Bos, M.; Jenck, F.; Martin, J. R.; Moreau, J. L.; Sleight, A. J.; Wichmann, J.; Widmer, U. Novel agonists of 5HT2C receptors. Synthesis and biological evaluation of substituted 2-(indol-1-yl)-1-methylethylamines and 2-(indeno[1,2-b]pyrrol-1-yl)-1methylethylamines. Improved therapeutics for obsessive compulsive disorder*, Journal of Medicinal Chemistry*, **1997**, *40*, 2762-2769.
27. Strauss WL, Kemper RR, Jayakar P, Kong CF, Hersh LB, Hilt DC, Rabin M "Human choline acetyltransferase gene maps to region 10q11-q22.2 by in situ hybridization". *Genomics*, **1991,** *9 (2)*: 396–8.

28. Bartus RT, Dean RL, Beer B, Lippa AS (30 July 1982). "The cholinergic hypothesis of geriatric memory dysfunction". Science. 217 (4558): 408–14.
29. Geula C, Mesulam MM, Saroff DM, Wu CK, Relationship between plaques, tangles, and loss of cortical cholinergic fibers in Alzheimer disease, *J Neuropathol Exp Neurol.,* **1998**, 57, 63–75.
30. Turkan, F.; Cetin, A.; Taslimi, P.; Gulcin, I. Some pyrazoles derivatives: Potent carbonic anhydrase, α-glycosidase, and cholinesterase enzymes inhibitors, *Arch. Pharm*. **2018**, 351.
31. Shaikh, S.; Dhavan, P.; Pavale, G.; Ramana, M.M.V.; Jadhav, B.L. Design, synthesis and evaluation of pyrazole bearing α-aminophosphonate derivatives as potential acetylcholinesterase inhibitors against Alzheimer's disease. *Bioorg. Chem.* **2020**, *96*, 103589–103611.
32. Gutti, G.; Kumar, D.; Paliwal, P.; Ganeshpurkar, A.; Lahre, K.; Kumar, A.; Krishnamurthy, S.; Singh, S.K. Development of pyrazole and spiropyrazoline analogs as multifunctional agents for treatment of Alzheimer's disease. *Bioorg. Chem.* **2019**, *90*, 103080.
33. Hochdorffer, K.; Marz-Berberich, J.; Nagel-Steger, L.; Epple, M.; Meyer-Zaika, W.; Horn, A.H.; Sticht, H.; Sinha, S.; Bitan, G.; Schrader, T. Rational design of β-sheet ligands against Aβ42-induced toxicity. *J. Am. Chem. Soc.* **2011**, *133*, 4348–4358.
34. Wagner, J.; Ryazanov, S.; Leonov, A.; Levin, J.; Shi, S.; Schmidt, F.; Prix, C.; Pan-Montojo, F.; Bertsch, U.; Mitteregger-Kretzschmar, G.; et al. Anle138b: A novel oligomer modulator for disease-modifying therapy of neurodegenerative diseases such as prion and Parkinson's disease. *Acta. Neuropathol.* **2013**, *125*, 795–813.
35. Wagner, J.; Krauss, S.; Shi, S.; Ryazanov, S.; Steffen, J.; Miklitz, C.; Leonov, A.; Kleinknecht, A.; Goricke, B.; Weishaupt, J.H.; et al. Reducing tau aggregates with anle138b delays disease progression in a mouse model of tauopathies. *Acta. Neuropathol.* **2015**, *130*, 619–631.
36. Matthes, D.; Gapsys, V.; Griesinger, C.; de Groot, B.L. Resolving the atomistic modes of anle138b inhibitory action on peptide oligomer formation. *ACS Chem. Neurosci.* **2017**, *8*, 2791–2808.
37. Fisher, D.A.; Smith, J.F.; Pillar, J.S.; St Denis, S.H.; Cheng, J.B. Isolation and characterization of PDE9A, a novel human cGMP-specific phosphodiesterase. *J. Biol. Chem.* **1998**, *273*, 15559–15564.
38. Kleiman, R.J.; Chapin, D.S.; Christoffersen, C.; Freeman, J.; Fonseca, K.R.; Geoghegan, K.F.; Grimwood, S.; Guanowsky, V.; Hajos, M.; Harms, J.F.; et al. Phosphodiesterase 9A regulates central cGMP and modulates responses to cholinergic and monoaminergic perturbation in vivo. *J. Pharmacol. Exp. Ther.* **2012**, *341*, 396–409.

39. Verhoest, P.R.; Fonseca, K.R.; Hou, X.; Proulx-Lafrance, C.; Corman, M.; Helal, C.J.; Claffey, M.M.; Tuttle, J.B.; Coffman, K.J.; Liu, S.; et al. Design and discovery of 6-[(3S,4S)-4-methyl-1-(pyrimidin-2-ylmethyl)pyrrolidin-3-yl]-1-(tetrahydro-2*H*-pyran-4-yl)-1,5-dihydro-4H-pyrazolo[3,4-*d*]pyrimidin-4-one (PF-04447943), a selective brain penetrant PDE9A inhibitor for the treatment of cognitive disorders. *J. Med. Chem.* **2012**, *55*, 9045–9054.
40. Schwam, E.M.; Nicholas, T.; Chew, R.; Billing, C.B.; Davidson, W.; Ambrose, D.; Altstiel, L.D. A multicenter, double-blind, placebo-controlled trial of the PDE9A inhibitor, PF-04447943, in Alzheimer's disease. *Curr. Alzheimer Res.* **2014**, *11*, 413–421.
41. Moschetti, V.; Boland, K.; Feifel, U.; Hoch, A.; Zimdahl-Gelling, H.; Sand, M. First-in-human study assessing safety, tolerability and pharmacokinetics of BI 409306, a selective phosphodiesterase 9A inhibitor, in healthy males. *Br. J. Clin. Pharmacol.* **2016**, *82*, 1315–1324.
42. Rosenbrock, H.; Giovannini, R.; Schanzle, G.; Koros, E.; Runge, F.; Fuchs, H.; Marti, A.; Reymann, K.G.; Schroder, U.H.; Fedele, E.; et al. The novel phosphodiesterase 9A inhibitor BI 409306 increases cyclic guanosine monophosphate levels in the brain, promotes synaptic plasticity, and enhances memory function in rodents. *J. Pharmacol. Exp. Ther.* **2019**, *371*, 633–641.
43. Pisani, L.; Catto, M.; Leonetti, F.; Nicolotti, O.; Stefanachi, A.; Campagna, F.; Carotti, A. Targeting monoamine oxidases with multipotent ligands: An emerging strategy in the search of new drugs against neurodegenerative diseases. *Cur. Med. Chem.* **2011**, *18*, 4568–4587.
44. Sterling, J.; Herzig, Y.; Goren, T.; Finkelstein, N.; Lerner, D.; Goldenberg, W.; Miskolczi, I.; Molnar, S.; Rantal, F.; Tamas, T.; et al. Novel Dual Inhibitors of AChE and MAO Derived from hydroxy aminoindan and phenethylamine as potential treatment for Alzheimer's disease. *J. Med. Chem.* **2002**, *45*, 5260–5279.
45. Huang, L.; Lu, C.; Sun, Y.; Mao, F.; Luo, Z.; Su, T.; Jiang, H.; Shan, W.; Li, X. Multitarget-directed benzylideneindanone derivatives: Anti-β-amyloid (Aβ) aggregation, antioxidant, metal chelation, and monoamine oxidase B (MAO-B) inhibition properties against Alzheimer's disease. *J. Med. Chem.* **2012**, *55*, 8483–8492.
46. Tzvetkov, N.T.; Antonov, L. Subnanomolar indazole-5-carboxamide inhibitors of monoamine oxidase B (MAO-B) continued: Indications of iron binding, experimental evidence for optimised solubility and brain penetration. *J. Enzyme Inhib. Med. Chem.* **2017**, *32*, 960–967.
47. Brand-Williams W, Cuvelier ME, Berset C; Use of a free radical method to evaluate antioxidant activity. *Lebensmittel- Wissencraft und- Technologie*, **1995**; *28*, 25-30.

48. Mensor LL, Menezes FS, Leitao GG, Reis AS, dos Santos TC, Coube CS, et al.. Screening of Brazilian plant extracts for antioxidant activity by the use of DPPH free radical method, *Phytotherapy Research*, **2001**, *15,* 127-130.

****